

## Effects of pH on Electrocatalytic Activity of Carbon Nanotubes in Poly(acrylic acid) Composites Used for Electrochemical Selective Detection of Uric Acid and Dopamine in the Presence of Ascorbic Acid

Yeong-Tarnng Shieh<sup>1,\*</sup>, Chi-Ming Wen<sup>2</sup>, Rong-Hsien Lin<sup>2</sup>, Tzong-Liu Wang<sup>1</sup>, Chien-Hsin Yang<sup>1</sup>, Yawo-Kuo Twu<sup>3</sup>

<sup>1</sup> Department of Chemical and Materials Engineering, National University of Kaohsiung, Kaohsiung 811, Taiwan

<sup>2</sup> Department of Chemical and Materials Engineering, National Kaohsiung University of Applied Sciences, Kaohsiung 807, Taiwan

<sup>3</sup> Department and Graduate Program of Bioindustry Technology, Dayeh University, Dacun, Changhua 515, Taiwan

\*E-mail: [yts@nuk.edu.tw](mailto:yts@nuk.edu.tw)

Received: 21 July 2012 / Accepted: 16 August 2012 / Published: 1 September 2012

---

Effects of pH on dispersion of carbon nanotubes (CNT) in poly(acrylic acid) (PAA) composites and on electrocatalytic activity of CNT toward oxidation reactions of uric acid (UA) at the composite-modified glassy carbon electrode (GCE) were investigated. Cyclic voltammetry data found that CNT in PAA could electrocatalyze the oxidation reactions of UA as indicated by a significant increase in the anodic peak current ( $I_{pa}$ ). Better dispersion of CNT in the PAA cast film exhibited a higher  $I_{pa}$  and electrocatalytic activity. The  $I_{pa}$  was increased with increasing CNT content, with the highest increasing rate from pH 7 at which the electrode was modified by the composite. For a given pH, CNT had higher electrocatalytic activity than fCNT (the functionalized CNT). In the presence of an excess of ascorbic acid, UA and dopamine (DA) could be simultaneously detected by the PAA/CNT 10/2.5 of pH 7-modified GCE. The sensitivity for simultaneous detection of DA was higher than that for UA. The linear range for the DA detection was 0.04–6  $\mu\text{M}$  and for the UA detection was 0.04–3  $\mu\text{M}$ .

---

**Keywords:** Carbon nanotubes, poly(acrylic acid), composite-modified electrode, electrocatalytic activity, simultaneous detection

### 1. INTRODUCTION

Uric acid (UA) is main final products of purine metabolism in the human body. UA and ascorbic acid (AA) coexist in blood and urine. It is not easy to selectively detect UA in the presence of

AA, due to similar oxidation potentials of UA and AA at bare electrodes [1]. Dopamine (DA) is an important catecholamine neurotransmitter in the central nervous, cardiovascular and hormonal systems because abnormal DA metabolism may lead to schizophrenia and Parkinson's disease [2]. The rapid and accurate determination of DA concentration in body fluid is therefore important to diagnose the diseases. However, DA also largely coexists with AA in the body fluid. The oxidation potential of AA is similar to that of DA due to homogeneous catalytic effect [3]. It would cause the overlapped voltammetric responses and be difficult to discriminate signals in electrochemical analysis. Therefore, it is of importance to distinguish DA from AA or eliminate the interference of AA. There have been intense investigations in the development of methods for the selective detections of DA, UA, and AA [4-14]. Although the simultaneous detection of DA, AA, and UA at polymer-modified electrodes has been reported [9-14], the detection was rarely reported at a pH sensitive carbon nanotubes (CNT) / poly(acrylic acid)(PAA) composite-modified electrode [1] with which the effects of pH on the detections were not investigated.

CNT is hydrophobic in nature [15, 16], easily dispersing in non- or low-polar solvents such as acetone and alcohol but precipitating in deionized water, a highly polar solvent [17]. With acid treatment, CNT can be functionalized by carboxylic groups (COOH) and exhibits hydrophilic properties, resulting in effective dispersion in deionized water but not in acetone or alcohol [17]. Since protonation and deprotonation of COOH groups depend on pH, the dispersion of acid-treated CNT in water is prone to change with pH. The dispersion of acid-treated CNT increases with a rise in pH in water. Previous studies [17-19] revealed that acid-treated CNT are poorly dispersed in low-pH water ( $\text{pH} \leq 3$ ) due to full protonation at this low pH, leading to aggregation by hydrogen bonding [19]. However, the aqueous solution at very high pH (e.g., pH 13) unexpectedly exhibits poor dispersion for acid-treated CNT [17] due to a higher ionic strength arising from a larger amount of sodium cations in the aqueous solution of pH 13 to cause the aggregation of carboxylate anions, which leads to precipitation.

PAA, a weak polyelectrolyte, is a water-soluble polymer and its conformation in water is sensitive to pH due to the presence of the ionizable COOH side group in every repeating unit. PAA was found to be a good dispersing agent for CNT at pH 5, a value close to the pKa of PAA [20]. PAA was reportedly grafted on CNT, and the resulting PAA-grafted CNT exhibit sound dispersion in water and other polar solvents [21]. The CNT microstructure varied with pH in PAA aqueous solutions [22]. At a low pH, PAA was highly coiled due to the hydrogen bonding of COOH groups, leading to aggregated CNT. At a high pH, on the other hand, PAA was extended due to the repulsion of negatively charged carboxylate anions, resulting in exfoliated CNT. PAA-wrapped CNT had been studied for their application as  $\beta$ -Nicotinamide adenine dinucleotide (NADH) sensors [23]. Liu et al. [23] observed that the PAA-CNT complex film-covered electrode had stable and excellent electrocatalytic activity for oxidizing NADH. Glassy carbon electrode (GCE) that was modified by PAA-coated CNT followed by binding ferrocene and glucose oxidase exhibited electrocatalytic activity for the oxidation of glucose [24]. As described earlier, the pH and ionic strength in aqueous solutions affected the microstructure of CNT in PAA and might consequently affect the electrocatalytic activity of CNT on PAA-modified electrodes. In this work, to develop an optimal electrode for sensing devices, how the pH-varied CNT dispersion in PAA affected the electrocatalytic

activity of CNT to redox reactions of UA was investigated. The selective and simultaneous detection of UA and DA in the presence of an excess of AA was also examined using the PAA/CNT-modified GCE.

## 2. EXPERIMENTAL

### 2.1 Materials

CNT was synthesized by thermal chemical vapor deposition at 750 °C for 1 h using acetylene as carbon source and ferrocene as catalyst in a quartz tube furnace in our laboratories [17]. The deposited product was investigated by transmission electron microscopy (TEM, JEOL JEM-1200CXII) and demonstrated to consist of multi-walled CNT. The synthesized CNT was approximately 20–30 nm in diameter and over 1 µm in length. The COOH-functionalized CNT (fCNT) was synthesized by acid treatment on raw CNT in a mixture of sulfuric acid and nitric acid at a ratio of 3/2 by volume at 60 °C for 3 h. PAA, with an average molecular weight of 100,000 g/mol, of 35 wt% in aqueous solution was supplied by Sigma-Aldrich and used as received. UA with purity of higher than 99 %, DA with purity of higher than 98 %, and AA with purity of higher than 99.7 % were all received from Sigma-Aldrich.

### 2.2 CNT and fCNT dispersions in PAA aqueous solutions of different pH

Aqueous solutions of different pH containing 0.1 wt% of PAA were prepared by adding HCl or NaOH. Various amounts of CNT (or fCNT) were added to obtain CNT (or fCNT) dispersions in PAA aqueous solutions of different pH after sonication for 10 min. The pH and x/y in the sample code PAA-pH/CNT x/y stand for the pH value of the PAA solution and the x/y for the weight ratio of PAA/CNT, respectively. The so prepared dispersions of PAA-pH/CNT x/y and PAA-pH/fCNT x/y were visually examined on the dispersion stability and recorded using a digital camera as a function of time. The dispersion, immediately after 10-min sonication, was cast on a precleaned glass plate followed by drying in a hood to examine surface morphology using a field emission scanning electron microscopy (FESEM, HITACHI S-4800). The FESEM was operated at 3 KeV.

### 2.3 Preparation of PAA/CNT- and PAA/fCNT-modified GC electrode

A 20 µL of the PAA-pH/CNT x/y or the PAA-pH/fCNT x/y dispersion taken immediately after sonication was cast on a prepolished glassy carbon electrode (GCE), followed by placing in a ventilated hood for about 12 h until the cast film on GCE was dry. The active area of the GCE for the cast film was a circle with 3 mm in diameter.

### 2.4 Electrochemical Analyses of PAA/CNT- and PAA/fCNT-modified GCE

A potentiostat (CH611D, CH Instruments) was used to conduct cyclic voltammetry (CV) analyses at 25 °C in a conventional three-electrode system with GCE as working electrode, a platinum

wire as auxiliary electrode, and an Ag/AgCl/3M KCl as reference electrode. The PAA-pH/CNT *x/y*– or the PAA-pH/fCNT *x/y*–modified GCE was immersed in 300 μM UA in 0.1 M KCl aqueous solution at 25 °C. The pH 7.4 phosphate buffer solution (0.1 M) served as a background electrolyte in all experiments. CV was conducted between 0 and 0.5 V with scan rate 100 mV/s. The second CV cycle was used for the investigations on electrocatalytic activity of the composite films. For simultaneous detection of DA and UA in the presence of a high AA content, the PAA-pH/CNT *x/y*– or the PAA-pH/fCNT *x/y*–modified GCE was immersed in the aqueous solution containing a mixture of the three analytes with UA and DA concentrations being in between 0 and 20 μM and AA being 300 μM, followed by CV analysis at 25 °C between 0 and 0.5 V with scan rate 100 mV/s.

### 3. RESULTS AND DISCUSSION

#### 3.1 Dispersions of CNT and fCNT in PAA aqueous solutions of different pH

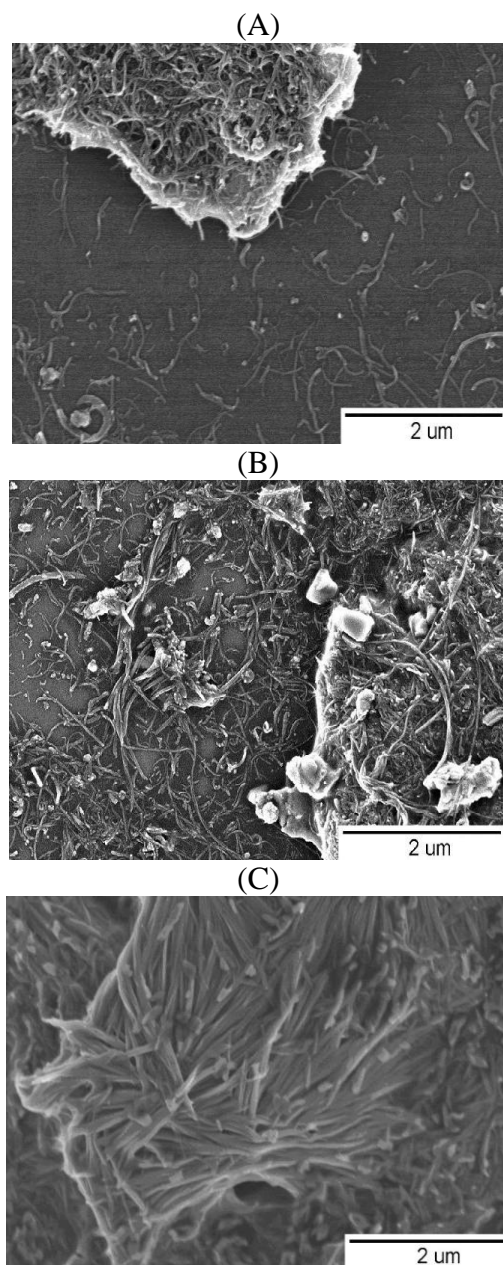
Sample Code	0 h	24 h	48 h
PAA-1/CNT 10/1			
PAA-3/CNT 10/1			
PAA-5/CNT 10/1			
PAA-7/CNT 10/1			
PAA-9/CNT 10/1			



**Figure 1.** Photos (taken immediately, 24 h, and 48 h after 10 min of sonication) of the PAA-pH/CNT 10/1 dispersion in 10 mL of water of different pH.

To investigate how dispersions of CNT and fCNT in PAA composites affected electrochemical properties of the composites-modified electrodes, CNT and fCNT dispersions in PAA aqueous solutions of different pH were first examined. As visually demonstrated in Figure 1, PAA helped improve the CNT dispersion over a wide pH range from 1 to 13 for at least 24 h. Without the presence of PAA, CNT precipitated immediately after sonication at any pH [25]. PAA solutions with low pH values (pH 1-5) and high pH values (pH 11 and 13) did not exhibit stable CNT dispersion for 48 h (Figure 1). The poor CNT dispersion in PAA aqueous solutions of low pH values could be attributed to the low extent of ionization (or deprotonation) of the COOH groups of PAA. The hydrogen bondings which were formed between COOH groups of PAA caused the aggregation of PAA, leading to precipitation of CNT. CNT exhibited good dispersion for 48 h in PAA solutions of pH 7 and 9; this could be attributed to the greater ionizations of COOH groups of PAA at these higher pH values, resulting in more carboxylate anions ( $-\text{COO}^-$ ), as compared to lower pH values. Negatively charged carboxylate anions on the PAA-coated CNT expelled one another to separate CNT, leading to good CNT dispersion. The unexpectedly poor CNT dispersions in PAA solutions of pH 11 and 13 were associated with high ionic strengths originating from the addition of NaOH used to increase pH. At these high pH values, a sizeable amount of NaOH was added, and the high content of sodium cations lent high ionic strength; this triggered the aggregation of carboxylate anions by ionic bonding, leading to precipitation [17]. Compared with PAA/CNT 10/1 (Figure 1), the PAA/fCNT 10/1 dispersion was stable for 48 h in solutions of pH 3–11 except pH 1 and 13 (photos not shown in this paper). The COOH-functionalized CNT (i.e., fCNT) exhibited good dispersion over a wider pH range as compared with CNT which was not functionalized.

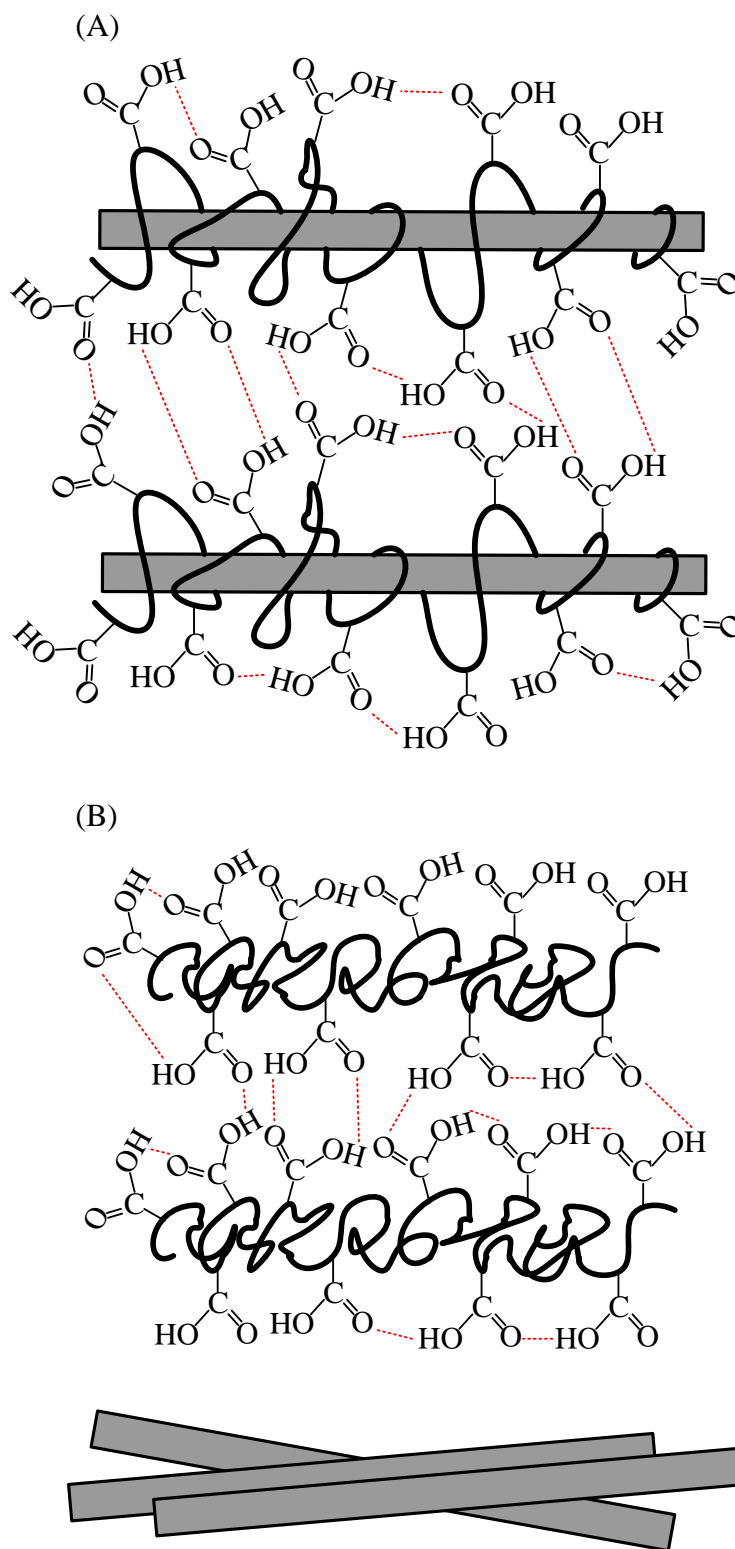
The FESEM image for the cast film from the PAA-1/CNT 10/1 solution (Figure 2A) could infer that most of CNT were coated by PAA to form aggregates (as schematically represented by Figure 3A) but some of CNT were not (Figure 3B). The aggregates arising from the PAA-coated CNT were loosened at pH 7 due to the expulsion of the negatively charged carboxylate anions on the PAA-coated CNT (Figure 2B).



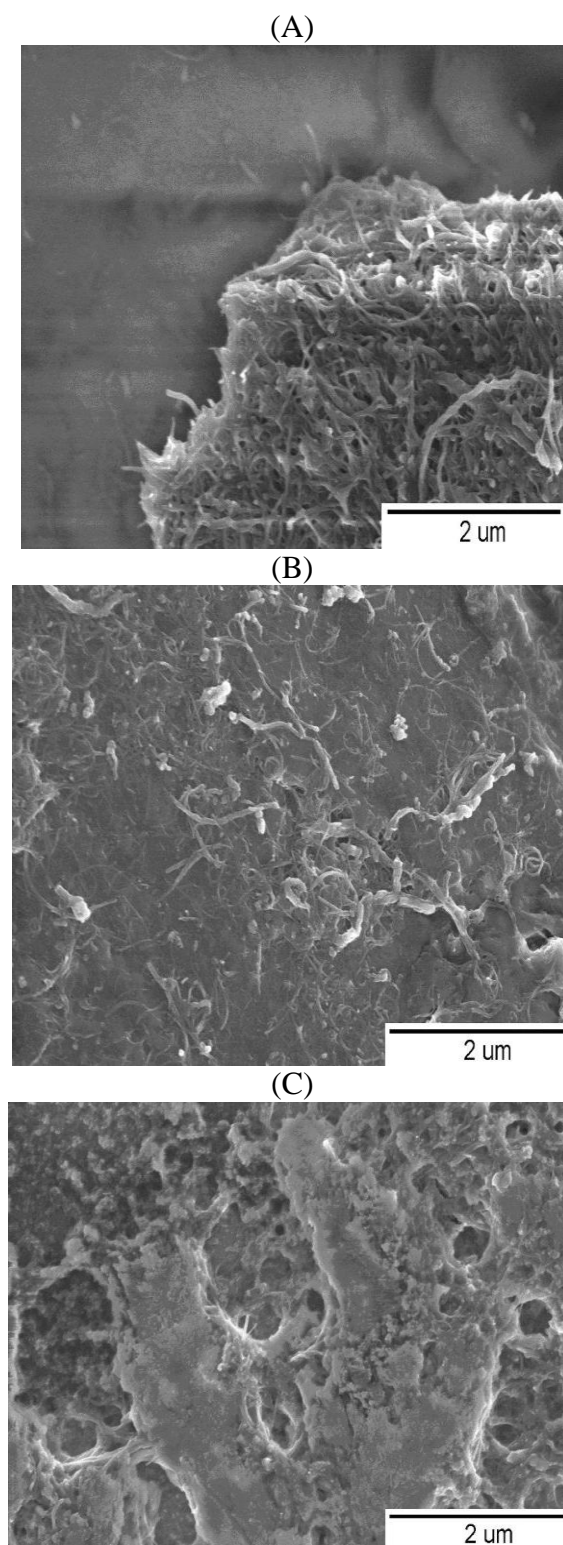
**Figure 2.** FESEM images for PAA/CNT 10/1 films that were cast from solutions of (A) pH 1, (B) pH 7, and (C) pH 13.

At pH 13, the carboxylate anions on the PAA-coated CNT formed ionic bonding with the  $\text{Na}^+$ , leading to aggregation and precipitation (Figure 2C). The findings in Figure 2 agreed with the visual observations for the CNT dispersion in PAA solutions of pH 1, 7, and 13 (Figure 1). The FESEM image for the cast film from the PAA-1/fCNT 10/1 solution (Figure 4A) could infer that all fCNT (CNT-COOH) were aggregated because hydrogen bondings were formed in PAA, in fCNT, and in between PAA and fCNT for both uncoated fCNT and PAA-coated fCNT (as schematically represented by Figure 5). Slightly loosened PAA/fCNT aggregates were found at pH 7 (Figure 4B) due to the expulsion of the formed negatively charged carboxylate anions. The aggregates were loosened further

but precipitated due to the ionic bondings formed between the carboxylate anions and the  $\text{Na}^+$  in PAA, in fCNT, and in between PAA and fCNT (Figure 4C).

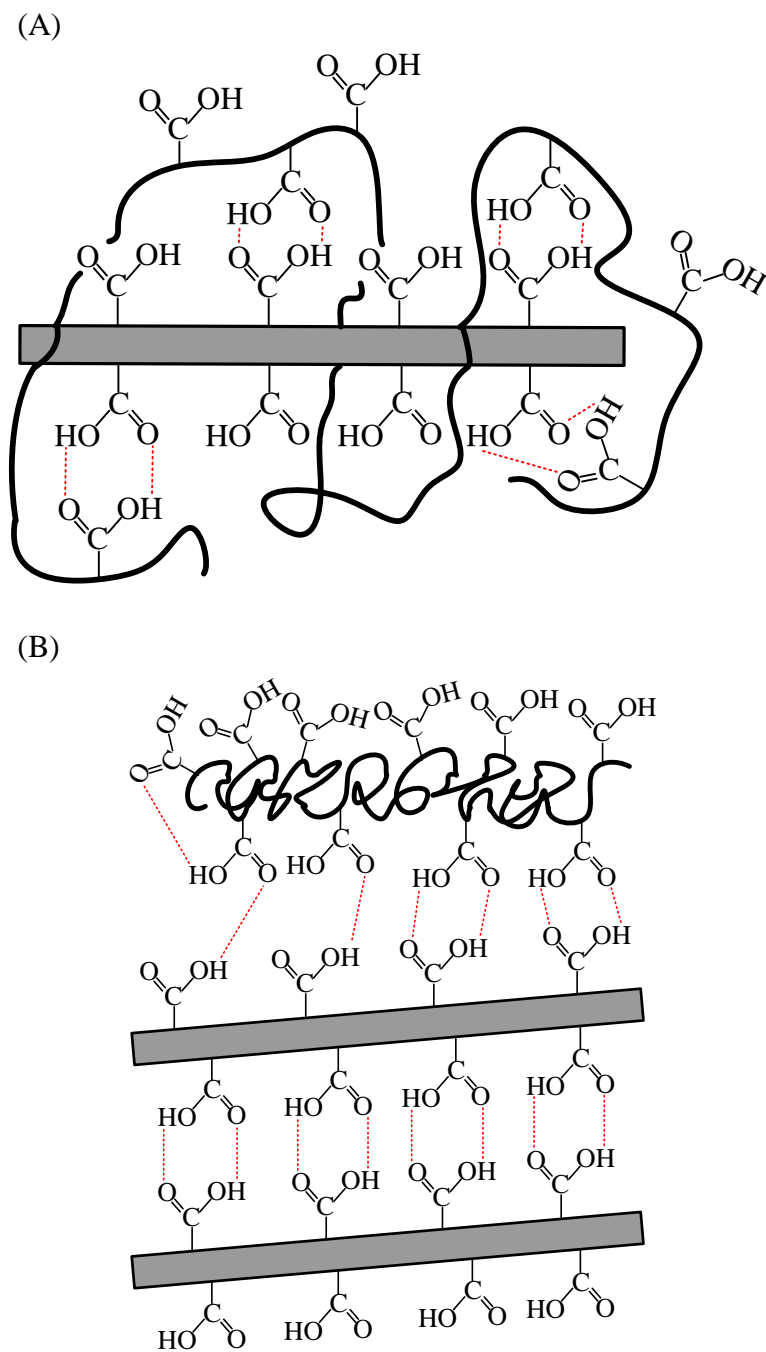


**Figure 3.** Schematic diagram of CNT dispersion in PAA solutions of  $\text{pH} < 5$  for (A) PAA-coated CNT, and (B) uncoated CNT. The dotted lines stand for hydrogen bondings.



**Figure 4.** FESEM images for PAA/fCNT 10/1 films that were cast from solutions of (A) pH 1, (B) pH 7, and (C) pH 13.

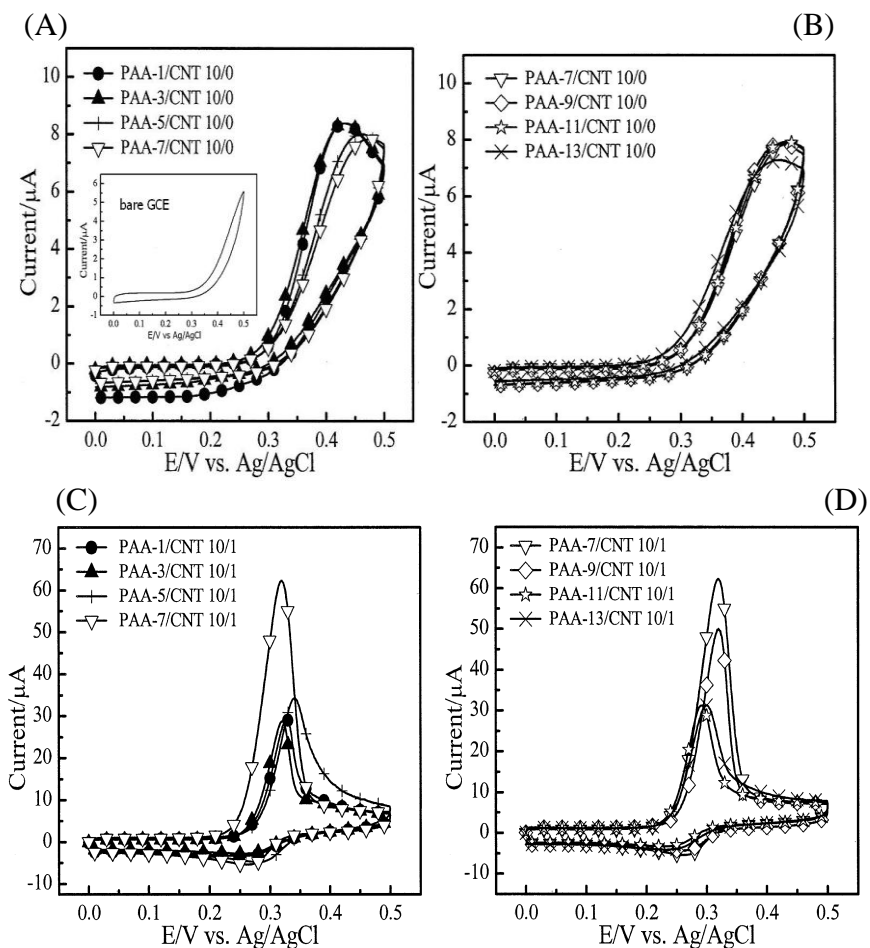
The surface morphologies at pH 13 in Figures 2C and 4C looked somewhat different because the ionic bonding did not form in CNT but did form in fCNT.



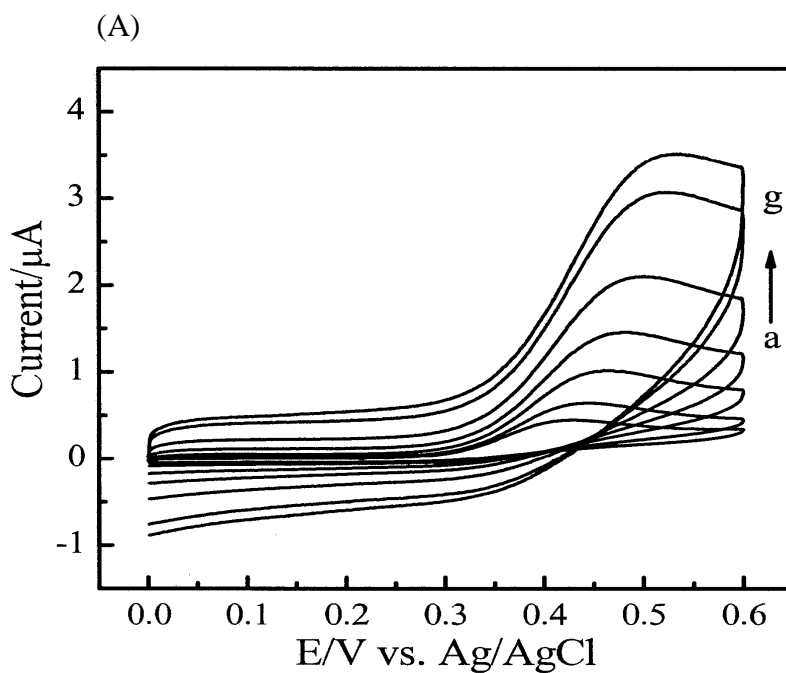
**Figure 5.** Schematic diagram of fCNT dispersion in PAA solutions of  $\text{pH} < 5$  for (A) PAA-coated fCNT, and (B) uncoated fCNT. The dotted lines stand for hydrogen bondings.

### 3.2 Cyclic voltammetric analyses of PAA/CNT composite films

Figures 6A and 6B show CV curves recorded at PAA-modified GCE in  $300 \mu\text{M}$  UA. As can be seen in these figures, without the presence of CNT, CV curves did not exhibit well defined anodic peaks, all with very low currents for all pH at which GCE was modified. In addition, cathodic peaks were not observed.



**Figure 6.** CV recorded at GCE, modified by (A, B) PAA-pH/CNT 10/0 and (C, D) PAA-pH/CNT 10/1, in 300 μM UA aqueous solution at pH 7.4 and 25 °C. Scan rate 100 mV/s.



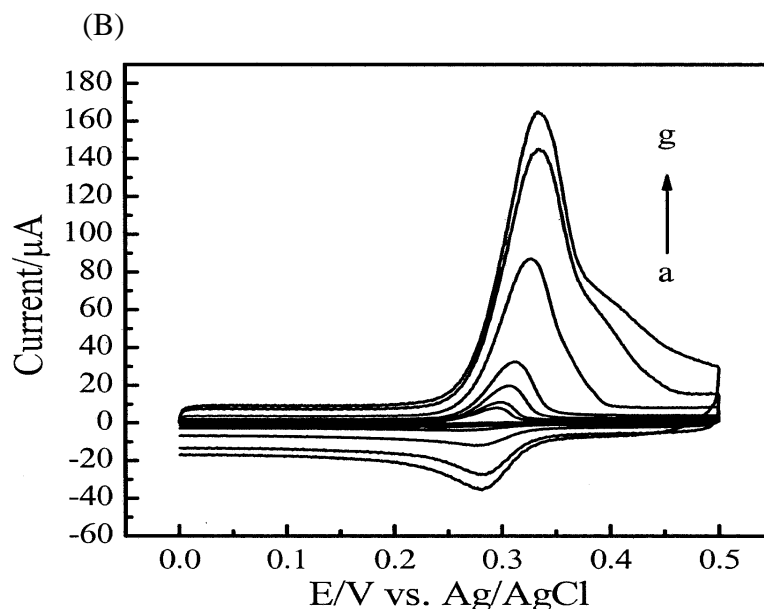


**Figure 7.** CVs of (A) PAA-7/CNT 10/0-modified GCE and (B) PAA-7/CNT 10/1-modified GCE in the presence of 50  $\mu\text{M}$  UA with varying scan rate. CVs were measured in 0.1 M phosphate buffer solution (pH 7.4). Scan rate (mV/s): (a) 10, (b) 20, (c) 40, (d) 100, (e) 200, (f) 400, and (g) 500.

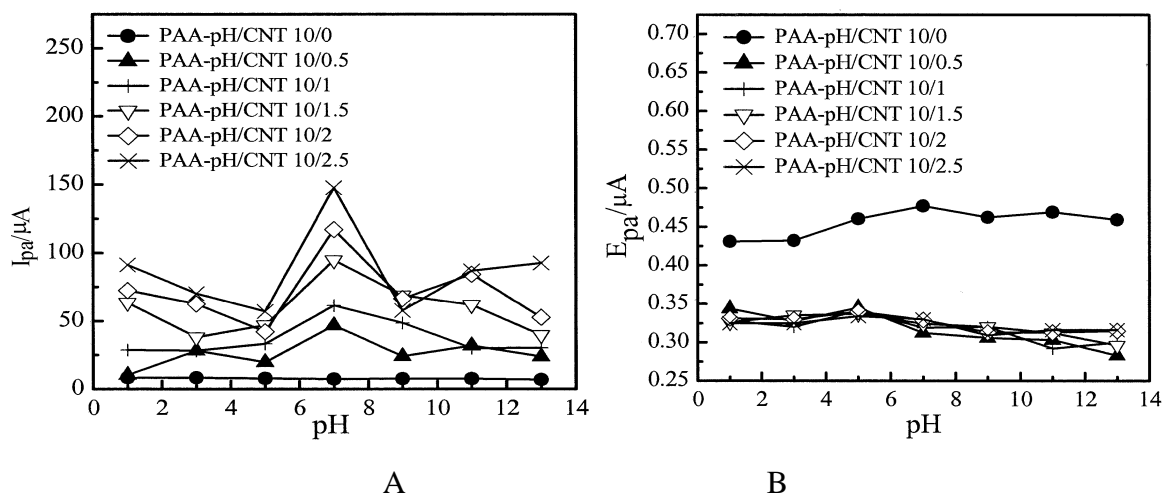


**Figure 8.** (A) Currents and (B) potentials of the anodic peaks ( $I_{pa}$  and  $E_{pa}$ , respectively) in CV, recorded at PAA-pH/CNT x/y-modified GCE in 300  $\mu\text{M}$  UA aqueous solution at pH 7.4 and 25  $^{\circ}\text{C}$ , as a function of pH at which the GCE was modified. Scan rate 100 mV/s.

CV curves in Figures 6C and 6D were recorded at PAA/CNT 10/1-modified GCE from aqueous solutions of different pH, all exhibiting well defined anodic peaks with much higher peak currents than those in Figures 6A and 6B. CV curves recorded at PAA/CNT of other ratios of composites-modified GCE including the ratios 10/0.5, 10/1.5, 10/2, and 10/2.5 were all giving rise to well defined anodic peaks as well but were not shown in this paper for clarity. Instead, their anodic

peak currents ( $I_{pa}$ ) were plotted as a function of pH and of the CNT/PAA ratio later in Figures 8 and 9, respectively. The much increased anodic peak currents with CNT present in the composites as shown in Figures 6C and 6D suggested that CNT exhibited electrocatalytic activity to the oxidation reactions of UA.

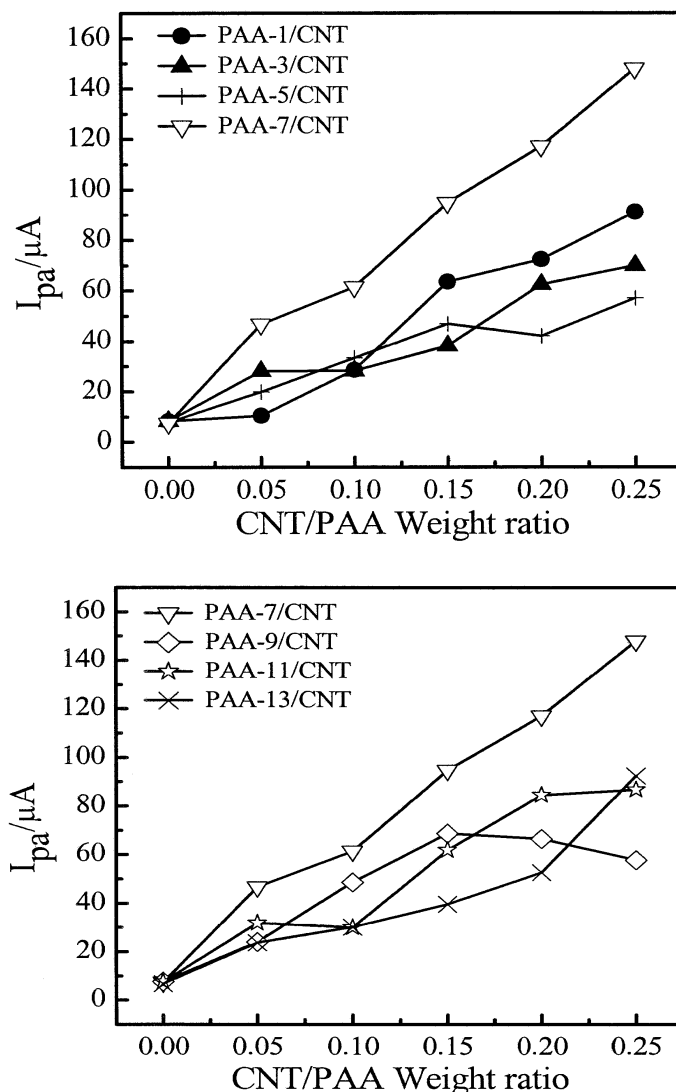


**Figure 9.** Currents of the anodic peaks ( $I_{pa}$ ) in CV, recorded at PAA-pH/CNT-modified GCE in 300  $\mu\text{M}$  UA aqueous solution at pH 7.4 and 25  $^{\circ}\text{C}$ , as a function of the CNT/PAA ratio. Scan rate 100 mV/s.

CV curves in Figure 6 did not clearly exhibit cathodic peaks, implying that the reduction reactions of UA were much slower than the oxidation reactions of UA, even with the catalysis of CNT (Figures 6C and 6D). Liu and coworkers [1] reported that the electro-oxidation of UA at PAA/GCE is irreversible and the anodic peak is rather broad, suggesting a slow electron-transfer kinetic. Another possibility for the missing cathodic peaks might be due to oxidative decomposition of UA during the oxidation scan. To investigate whether the oxidative decomposition of UA was a cause, varying CV

scan rates were conducted as shown in Figure 7. Given that a higher scan rate has a less time for the oxidative decomposition, cathodic peak is more likely to appear in a CV curve of a higher scan rate if the oxidative decomposition reaction is to occur. As can be seen in Figure 7A, the anodic peaks appeared at potentials at near 0.5 V which was high to lead to oxidative decomposition of UA, although the higher scan rates (200, 400, and 500 mV/s) than the scan rate of 100 mV/s used in Figure 6 did not give rise to cathodic peaks for PAA-7 modified GCE. From Figure 7B, however, the higher scan rates gave rise to cathodic peaks with peak currents increasing with increasing scan rates, revealing that the oxidative decomposition was a dominant cause for the observation of negligible cathodic peaks in Figure 6. Liu and coworkers [1] also reported that only anodic peak can be observed at low scan rates but, when the scan rate increased, the cathodic peak appeared and increased readily. They [1] explained that a relative higher scan rate can improve the electron-transfer reaction of UA oxidized at PAA/CNT-modified GCE. The  $I_{pa}$  values linearly increased with the root square of scan rates in Figure 7A suggested that the electron transfer for UA at PAA-7 modified GCE was diffusion-controlled whereas the  $I_{pa}$  values linearly increased with the scan rates in Figure 7B suggested a adsorption-controlled mechanism for UA at PAA-7/CNT 10/1-modified GCE.

The cast film from aqueous solution of pH 7 exhibited the greatest anodic peak intensity in Figures 6C and 6D, an indication that the more stable CNT dispersion in PAA solution (Figure 1) and the more uniform PAA/CNT cast film (Figure 2) would give the greater anodic peak intensity. As long as the PAA/CNT composite was cast at pH 7, the composite had the strongest anodic peak irrespective of the CNT content in the composite (Figure 8A). From Figure 8B, for all pH studied, the anodic peak potentials for the PAA/CNT composite films were all lower than those for the pure PAA films, indicating again that CNT exhibited electrocatalytic activity [26] to the redox reactions of UA. The effects of CNT contents in the PAA/CNT composite films that were cast at different pH on the anodic peak currents ( $I_{pa}$ ) could be clearly seen in Figure 9 in which the  $I_{pa}$  exhibited an increasing trend with increasing CNT content for a given pH, with the highest increasing rate for pH 7. This indicated that higher CNT contents exhibited higher electrocatalytic activities toward redox reactions of UA.

### 3.3 Cyclic voltammetric analyses of PAA/fCNT composite films

CV curves recorded at PAA/fCNT 10/1-modified GCE in 300  $\mu$ M UA were shown in Figure 10 and all exhibited much lower anodic peak currents than those for PAA/CNT 10/1 as in Figure 6. It was evident that the functionalized CNT (i.e., fCNT) did not exhibit as high electrocatalytic activity as CNT, although fCNT was more effective to be dispersed in PAA aqueous solution than CNT at a given pH. This might be associated with the structural damages on fCNT caused by the acid treatments. These structural damages interrupted the length of conjugated double bonds and decreased the delocalizations of electrons on CNT, leading to decreased electron transfer rates during oxidation reactions of UA. The PAA/fCNT 10/1 films cast at low pHs exhibited lower anodic peak currents ( $I_{pa}$ ) but higher anodic peak potentials ( $E_{pa}$ ) than those cast at high pHs (Figure 11), indicating that the PAA/fCNT composite prepared at higher pHs could give higher electrocatalytic activities to the

oxidation reactions of UA. This might be associated with the higher amount of carboxylate anions that could form on fCNT in the composite films as prepared at higher pHs, leading to having more interactions with the four secondary amine groups on UA, than those prepared at lower pHs.

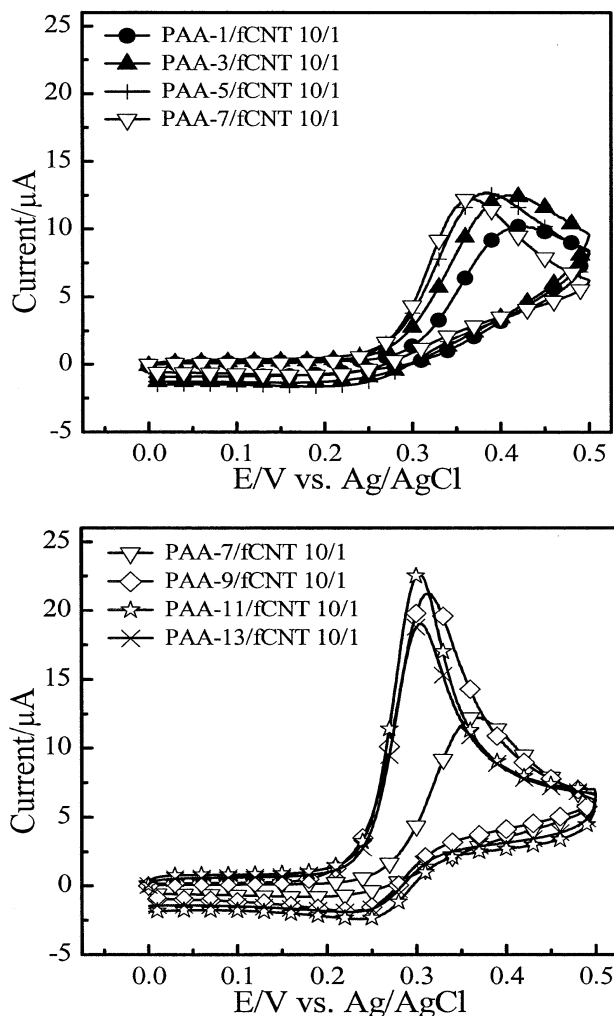


**Figure 10.** CV recorded at GCE, modified by PAA-pH/fCNT 10/1, in 300 μM UA aqueous solution at pH 7.4 and 25 °C. Scan rate 100 mV/s.

As can be also seen from Figure 11, the PAA/CNT 10/1 and PAA/fCNT 10/1 films both exhibited higher anodic peak currents and lower anodic potentials than the pure PAA films at any pH. This again demonstrated that CNT and fCNT were both able to electrocatalyze the oxidation reactions of UA, with CNT having a higher electrocatalytic capacity than fCNT.

### 3.4 Simultaneous detection of UA and DA in the presence of AA

In an attempt to investigate whether the PAA/CNT and PAA/fCNT composites could simultaneously detect UA and DA in the presence of an excess of AA, the PAA-7/CNT 10/2.5-

modified GCE which exhibited the strongest electrocatalytic activity (Figure 9) among all composites-modified GCE was chosen for the investigation.

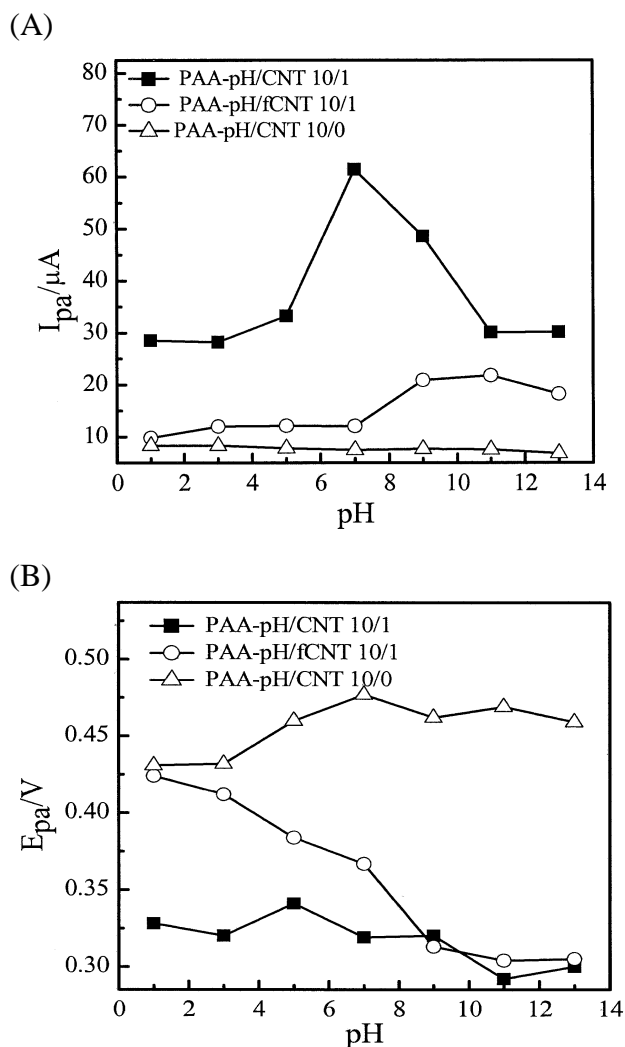


**Figure 11.** (A) Currents and (B) potentials of the anodic peaks ( $I_{pa}$  and  $E_{pa}$ , respectively) in CV, recorded at PAA-pH/CNT 10/0-, PAA-pH/CNT 10/1- and PAA-pH/fCNT 10/1-modified GCE in 300  $\mu M$  UA aqueous solution at pH 7.4 and 25  $^{\circ}C$ , as a function of pH at which the GCE was modified. Scan rate 100 mV/s.

Figure 12A shows CV curves recorded at PAA-7/CNT 10/2.5-modified GCE in aqueous solutions of a mixture of DA (0–20  $\mu M$ ), UA (0–20  $\mu M$ ), and AA (300  $\mu M$ ). Two anodic peaks at near 0.16 and 0.3 V were observed and assigned to the oxidation reactions of DA and UA, respectively, as determined by prior analyses of the pure analytes. As can be seen in Figure 12A, in the presence of a high AA content (300  $\mu M$ ), the anodic peak currents of UA and DA, starting from background currents at 3.2  $\mu A$  for the DA peak and 3.9  $\mu A$  for the UA peak, were found to increase with increasing concentrations. It was thus evident that DA and UA could be simultaneously detected by the PAA/CNT composite-modified GCE in the presence of a high AA content. The reduction reactions of

UA could not be clearly seen whereas those of DA could be seen for high concentrations (Figure 12A), an indication that DA had a higher reduction reaction rate and/or was more stable to resist oxidative decomposition than UA.

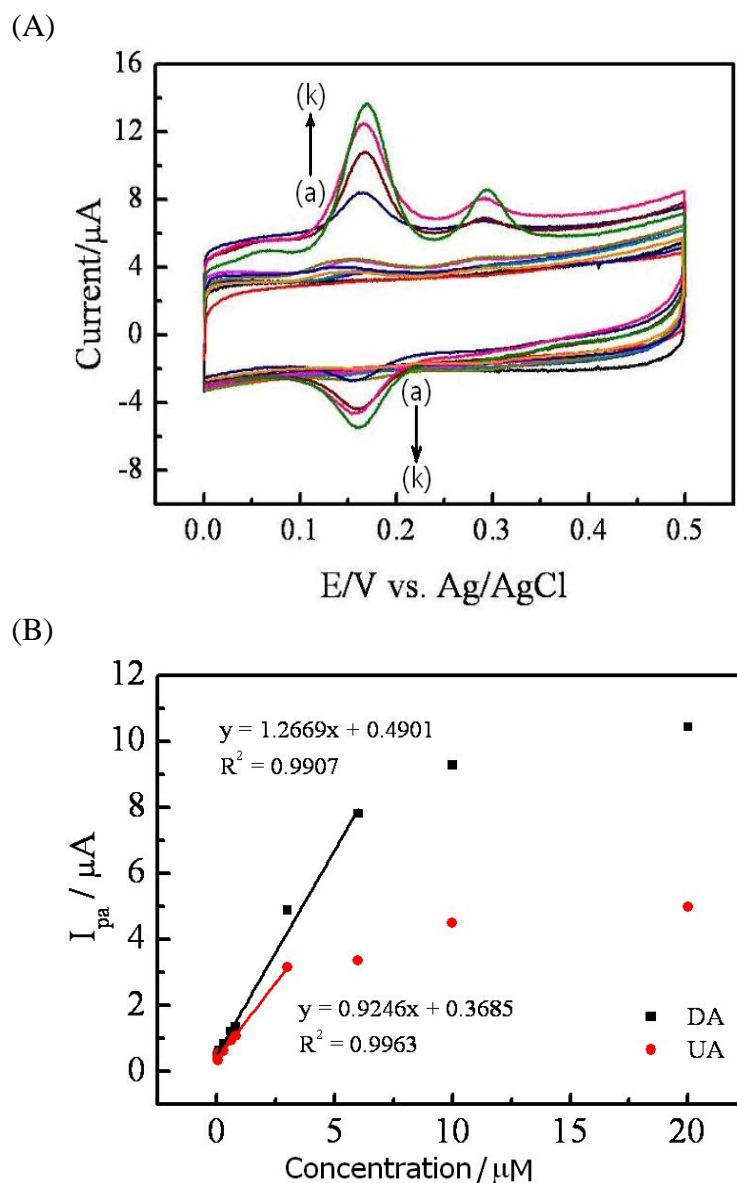


**Figure 12.** (A) CV recorded at PAA-7/CNT 10/2.5-modified GCE in aqueous solutions of a mixture of DA (0–20  $\mu\text{M}$ ), UA (0–20  $\mu\text{M}$ ), and AA (300  $\mu\text{M}$ ) at pH 7.4 and 25  $^{\circ}\text{C}$ . Scan rate 100 mV/s. (B) Anodic peak currents ( $I_{pa}$ ) of CV from (A) as a function of concentration of DA and UA: (a) 0  $\mu\text{M}$ , (b) 0.04  $\mu\text{M}$ , (c) 0.06  $\mu\text{M}$ , (d) 0.1  $\mu\text{M}$ , (e) 0.3  $\mu\text{M}$ , (f) 0.6  $\mu\text{M}$ , (g) 0.8  $\mu\text{M}$ , (h) 3  $\mu\text{M}$ , (i) 6  $\mu\text{M}$ , (j) 10  $\mu\text{M}$ , and (k) 20  $\mu\text{M}$ .

The sensitivity for simultaneous detection of DA was higher than that for UA (Figure 12B). The linear range for the DA detection was 0.04–6  $\mu\text{M}$  and for the UA detection was 0.04–3  $\mu\text{M}$ . The sensitivity for the DA detection was 1.267  $\mu\text{A}/\mu\text{M}$  (or 17.93  $\mu\text{A}/\text{cm}^2 \mu\text{M}$  by taking the circled active

area with 3 mm in diameter on GCE into consideration) and for the UA detection was  $0.925 \mu\text{A}/\mu\text{M}$  (or  $13.09 \mu\text{A}/\text{cm}^2 \mu\text{M}$ ).

#### 4. CONCLUSIONS

Visual observations found that CNT exhibited good dispersions in PAA solutions of pH 7 and 9, but poor dispersions in PAA solutions of low pHs (pH 1-5) and high pHs (pH 11 and 13). FESEM images for surfaces of the films that were cast from the PAA/CNT dispersions of different pH were consistent with the visual observations for these dispersions. As compared to PAA-modified GCE, CV curves recorded at PAA/CNT composite-modified GCE exhibited well defined anodic peaks with significant increased peak currents for oxidation reactions of UA, indicating that CNT exhibited electrocatalytic activity toward oxidation reactions of UA. The more stable CNT dispersions in PAA solutions that could lead to the more uniform CNT dispersions in the cast films could result in the higher electrocatalytic activity. For a given pH at which the electrode was modified by the composite, the anodic peak current was found to increase with increasing CNT content, with the highest increasing rate for pH 7. The functionalized CNT (i.e., fCNT) did not exhibit electrocatalytic activity as high as CNT. In the presence of a high AA content, UA and DA could be simultaneously detected by the PAA-7/CNT 10/2.5 composite-modified GCE. The sensitivity for simultaneous detection of DA was higher than that for UA. The linear range for the DA detection was  $0.04\text{--}6 \mu\text{M}$  and for the UA detection was  $0.04\text{--}3 \mu\text{M}$ .

#### ACKNOWLEDGMENT

We gratefully acknowledge the financial support of the National Science Council of Taiwan under the contract NSC 98-2221-E-390-002-MY3.

#### References

1. A. Liu, I. Honma, H. Zhou, *Biosens. Bioelectron.*, 23 (2007) 74–80.
2. J.W. Mo, B. Ogorevc, *Anal. Chem.*, 73 (2001) 1196–1202.
3. M. A. Dayton, A. G. Ewing, R. M. Wightman, *Anal. Chem.*, 52 (1980) 2392–2396.
4. C. Y. Li, Y. J. Cai, C. H. Yang, C. H. Wu, Y. Wei, T. C. Wen, T. L. Wang, Y. T. Shieh, W. C. Lin, W. J. Chen, *Electrochimica Acta*, 56 (2011) 1955–1959.
5. H. R. Zare, N. Rajabzadeh, N. Nasirizadeh, M. Mazloum Ardakani, *J. Electroanal. Chem.*, 589 (2006) 60–69.
6. H. R. Zare, N. Nasirizadeh, M. Mazloum Ardakani, *J. Electroanal. Chem.*, 577 (2005) 25–33.
7. A. Safavi, N. Maleki, O. Moradlou, F. Tajabadi, *Anal. Biochem.*, 359 (2006) 224–229.
8. Y. Zhao, Y. Gao, D. Zhan, H. Liu, Q. Zhao, Y. Kou, Y. Shao, M. Li, Q. Zhuang, Z. Zhu, *Talanta*, 66 (2005) 51–57.
9. J. M. Zen, J. J. Jou, G. Ilangovan, *Analyst*, 123 (1998) 1345–1350.
10. J. W. Mo, B. Ogorevc, *Anal. Chem.*, 73 (2001) 1196–1202.
11. R. Aguilar, M. M. Davila, M. P. Elizalde, J. Mattusch, R. Wennrich, *Electrochimica Acta*, 49 (2004) 851–859.

12. H. S. Wang, T. H. Li, W. L. Jia, H. Y. Xu, *Biosens. Bioelectron.*, 22 (2006) 664–669.
13. T. Selvaraju, R. Ramaraj, *Electrochemistry Communications*, 5 (2003) 667–672.
14. Y. Li, X. Lin, *Sensors and Actuators B*, 115 (2006) 134–139.
15. J. H. Walther, R. L. Jaffe, E. M. Kotsalis, T. Werder, T. Halicioglu, P. Koumoutsakos, *Carbon*, 42 (2004) 1185–1194.
16. S. Niyogi, E. Bekyarova, M. E. Itkis, J. L. McWilliams, M. A. Hamon, R. C. Haddon, *J. Amer. Chem. Soc.*, 128 (2006) 7720–7721.
17. Y. T. Shieh, G. L. Liu, H. H. Wu, C. C. Lee, *Carbon*, 45 (2007) 1880–1890.
18. W. Zhao, C. Song, P. E. Pehrsson, *J. Amer. Chem. Soc.*, 124 (2002) 12418–12419.
19. L. Zeng, L. Zhang, A. R. Barron, *Nano Letters*, 5 (2005) 2001–2004.
20. K. Saint-Aubin, P. Poulin, H. Saadaoui, M. Maugey, C. Zakri, *Langmuir*, 25 (2009) 13206–13211.
21. S. Chen, G. Wu, Y. Liu, D. Long, *Macromolecules*, 39 (2006) 330–334.
22. J. C. Grunlan, L. Liu, Y. S. Kim, *Nano Letters*, 6 (2006) 911–915.
23. A. Liu, T. Watanabe, I. Honma, J. Wang, H. Zhou, *Biosens. Bioelectron.*, 22 (2006) 694–699.
24. Y. M. Yan, I. Baravik, O. Yehezkeli, I. Willner, *J. Phys. Chem. C*, 112 (2008) 17883–17888.
25. Y. T. Shieh, H. M. Wu, Y. K. Twu, Y. C. Chung, *Colloid Polymer Science*, 288 (2010) 377–385.
26. M. Musameh, J. Wang, M. Arben, Y. Lin, *Electrochemistry Communications*, 4 (2002) 743–746.